Qeios

Electron Spin Topology in Excited States and Fractional Spin Effect

Ju Gao and Fang Shen

Preprint v3

Aug 4, 2023

https://doi.org/10.32388/G5U3I5.3

Electron Spin Topology in Excited States and Fractional Spin Effect

Ju Gao* and Fang Shen
University of Illinois, Department of Electrical and Computer Engineering, Urbana, 61801, USA
(Dated: August 5, 2023)

The wave nature of the electron spin is shown by a multi-vortex current density topology in the excited states that is holographic in nature. When the wave spin interacts with a magnetic field smaller in size than the wave itself, fractional spin effect can be observed. The anomalous Zeeman splitting is shown to have a finer structure determined by the geometric factors and quantum numbers of the states.

I. ELECTRON SPIN DESCRIBED BY CURRENT DENSITY

Spin is a quantum mechanical property of an electron that represents the electron's internal angular momentum. However, what actually spins remains an open question, since the particle spin interpretation would require the electron to spin faster than the speed of light. Without a tangible physical explanation, spin is mostly accepted as an abstract two-valuedness property of the electron. Yet in electromagnetism, all charge behavior is fully described by the Lorentz covariant four-current $j = (c\rho, \boldsymbol{j})$, where ρ and $\boldsymbol{j}$ stand for the charge and current densities that are responsible for both the generation and interaction of an electromagnetic field. In quantum mechanics, the electron charge is described by the charge density calculated from the wavefunction, then the question is could the spin be described by the current density calculated by the same wavefunction?

In a recent paper [1], we have shown that a stable circulating current density exists for a Dirac electron in a quantum well without a magnetic field. We calculated the four current $j = (c\rho, \boldsymbol{j})$ from the wavefunction solution $\psi(x)$ of the Dirac equation by

$$\begin{aligned} \rho(x) &= \mathrm{e}\bar{\psi}(x)\gamma^0\psi(x) \\ \boldsymbol{j}(x) &= \mathrm{ec}\bar{\psi}(x)\boldsymbol{\gamma}\psi(x), \end{aligned} \tag{1}$$

where $\gamma^0, \boldsymbol{\gamma}$ are $\gamma-$matrix operators. The current density is shown to form a spinning vortex around the center of the charge density, often referred to as an electron cloud. In other words, the entire electron wave, or the electron cloud, spins.

Essentially, this is the wave spin interpretation that was first proposed by Belinfante [2, 3] who argued that spin should be regarded as a circulating flow of energy of the electron field. Ohanian [4] further elaborated the connection between the circulating momentum density and current density with the electron spin and the magnetic moment. Gao [1] showed that a confined electron has a stable circulating current density, but the wave packet of a free electron discussed by Ohanian is not stable and de-coherences quickly because the wavepacket is not constructed by a pure state.

* jugao2007@gmail.com

In essence the wave spin picture argues that the electron spin is not a local property pertaining to the particle electron, but a global property of the electron wave that has a tangible physical explanation in the spinning current density. To show that the electron wave spins intrinsically, we derive explicit expressions for the momentum and current densities of an electron in an eigenstate wavefunction Ψ of the Dirac equation, where $i\hbar\frac{\partial}{\partial t}\Psi = \mathcal{E}\Psi$ and $\mathcal{E}$ is the eigen energy,

$$\begin{aligned} \boldsymbol{j} &= \frac{ec^2}{\mathcal{E}}\left\{\boldsymbol{\nabla}\times\left(\Psi^\dagger\frac{\hbar}{2}\boldsymbol{\Sigma}\Psi\right) + i\frac{\hbar}{2}\left[\left(\boldsymbol{\nabla}\Psi^\dagger\right)\Psi - \Psi^\dagger\left(\boldsymbol{\nabla}\Psi\right)\right]\right\}, \\ \boldsymbol{G} &= \left\{\frac{1}{2}\boldsymbol{\nabla}\times\left(\Psi^\dagger\frac{\hbar}{2}\boldsymbol{\Sigma}\Psi\right) + i\frac{\hbar}{2}\left[\left(\boldsymbol{\nabla}\Psi^\dagger\right)\Psi - \Psi^\dagger\left(\boldsymbol{\nabla}\Psi\right)\right]\right\}. \end{aligned} \tag{2}$$

The above equations show that both the current density $\boldsymbol{j}$ and the momentum density $\boldsymbol{G}$ contain the spin term $\frac{\hbar}{2}\boldsymbol{\Sigma}$ with the spin operator $\boldsymbol{\Sigma}$ and the translational term with the momentum operator $-i\hbar\boldsymbol{\nabla}$. It is worth noting that these expressions are derived from separate origins. The momentum density is derived from a symmetrical energy-momentum tensor known as the Belinfante-Rosenfeld tensor [5]. This symmetrical tensor is constructed to serve as a source for the gravitational field as required by general relativity. The current density, on the other hand, is derived by using the Gordon decomposition and current density definition $\boldsymbol{j}(\boldsymbol{x}) = ec\Psi^\dagger(\boldsymbol{x})\boldsymbol{\alpha}\Psi(\boldsymbol{x})$ that ensures the conservation of charge. Here $\boldsymbol{\alpha}$ is the $\alpha-$matrix used in the Dirac equation. The momentum and current densities thus independently describe the mechanical and electrical spinning nature of the wave, with a factor of $\frac{1}{2}$ in the momentum expression that accounts for the gyromagnetic ratio $g = 2$ for the Dirac field.

We choose to focus our attention on the current density rather than the momentum density, because the wave spin manifests itself by the current density interacting with an electromagnetic field

$$jA = \rho\phi + \boldsymbol{j}\cdot\boldsymbol{A}. \tag{3}$$

The above equation accounts for all electromagnetic interactions for both classical and quantum electrodynamics. In this work, we will show that the current-field interaction jA not only recovers the conventional spin-field interaction, but also reveals geometric and topological effects that are absent in the particle spin picture, particularly for the electron in the excited states.

II. WAVE SPIN IN EXCITED STATES

To investigate the wave spin in the excited states of a confined electron, we first seek the exact solution of the Dirac equation

$$i\hbar\frac{\partial}{\partial t}\Psi(\boldsymbol{r},t)=\left[c\boldsymbol{\alpha}\cdot(-i\hbar\boldsymbol{\nabla})+\gamma^0\mathrm{mc}^2+U(\boldsymbol{r})\right]\Psi(\boldsymbol{r},t), \tag{4}$$

in a two-dimensional quantum well

$$U(\boldsymbol{r})=U(x,y)=\begin{cases}0,-L_x<x<L_x,-L_y<y<L_y\\ \infty,\text{elsewhere.}\end{cases} \tag{5}$$

The four-component spinor wavefunction is expressed by the separation of the temporal and z-coordinate variables

$$\Psi(\boldsymbol{r},t)=Ne^{-i\mathcal{E}t/\hbar}e^{iP_zz/\hbar}\begin{pmatrix}\mu_A(x,y)\\ \mu_B(x,y)\end{pmatrix}, \tag{6}$$

where $\mathcal{E}$ is the energy, P_z is the momentum along z-direction, and $\mu_A(x,y)$ and $\mu_B(x,y)$ are two-component spinor wavefunctions.

We now plug Eq. 6 into the Dirac equation Eq. 4 and set $P_z=0$ since it does not contribute to the spin. We thus obtain the coupled equations

$$\begin{aligned}\left(\mathcal{E}-mc^2\right)\mu_A(x,y) &= -i\hbar c\left(\sigma_x\frac{\partial}{\partial x}+\sigma_y\frac{\partial}{\partial y}\right)\mu_B(x,y);\\ \left(\mathcal{E}+mc^2\right)\mu_B(x,y) &= -i\hbar c\left(\sigma_x\frac{\partial}{\partial x}+\sigma_y\frac{\partial}{\partial y}\right)\mu_A(x,y),\end{aligned} \tag{7}$$

where σ_x and σ_y are the Pauli matrices.

Eqs. 7 is combined to obtain a second-order differential equation for $\mu_A(x,y)$

$$\left(\mathcal{E}^2-m^2c^4\right)\mu_A(x,y)=-\hbar^2c^2\left(\frac{\partial^2}{\partial x^2}+\frac{\partial^2}{\partial y^2}\right)\mu_A(x,y), \tag{8}$$

whose eigensolution for the spin-up electron is found

$$\mu_A(x,y)=\sin[k_x(x+L_x)]\sin[k_y(y+L_y)]\begin{pmatrix}1\\0\end{pmatrix}, \tag{9}$$

where $k_x=\frac{\pi n_x}{2L_x};k_y=\frac{\pi n_y}{2L_y}$ are the wave vectors and n_x, $n_y=1,2,3...$ are the quantum numbers of the eigen states. The eigen energy

$$\mathcal{E}=mc^2\sqrt{1+\eta^2} \tag{10}$$

is quantized by n_x and n_y according to the expression of a dimensionless geometric factor

$$\eta=\sqrt{n_x^2\left(\frac{\lambda_c}{4L_x}\right)^2+n_y^2\left(\frac{\lambda_c}{4L_y}\right)^2} \tag{11}$$

that measures the dimensions of the quantum well (L_x,L_y) against the reduced Compton wavelength $\lambda_c=\frac{\hbar}{mc}$ at different states (n_x,n_y).

The wavefunction $\mu_B(x,y)$ is subsequently derived via Eq. 7 as derivative of $\mu_A(x,y)$, where it can be observed that $\mu_B(x,y)$ does not vanish at the walls. The same discontinuity of the wavefunction derivative occurs for the Schrödinger electron in the infinite quantum well. This is a consequence of using the unrealistic infinite potential and enforcing a total collapse of wavefunction outside the well. A more realistic potential and inclusion of the tunnelling wavefunction outside the well will fix the derivative discontinuity, and here the infinite quantum well is adopted to offer clear analytical expressions and insights for our discussions. Moreover, it can be shown that the basic law of charge conservation is obeyed everywhere in the well by combining Eqs. 7 and 1 to give,

$$\frac{\partial}{\partial t}\rho+\boldsymbol{\nabla}\cdot\boldsymbol{j}=0. \tag{12}$$

The complete four-component spinor wavefunction is then obtained

$$\Psi(\boldsymbol{r},t)=Ne^{-i\mathcal{E}t/\hbar}\begin{pmatrix}\sin[k_x(x+L_x)]\sin[k_y(y+L_y)]\\ 0\\ 0\\ -i\frac{\eta_x}{1+\sqrt{\eta^2+1}}\cos[k_x(x+L_x)]\sin[k_y(y+L_y)]+\frac{\eta_y}{1+\sqrt{\eta^2+1}}\sin[k_x(x+L_x)]\cos[k_y(y+L_y)]\end{pmatrix}. \tag{13}$$

where $\eta_x=\frac{\hbar k_x}{mc},\eta_y=\frac{\hbar k_y}{mc}$ are dimensionless factors along x and y directions. The normalization factor of the wavefunction is found

$$N=\sqrt{\frac{1+\sqrt{1+\eta^2}}{\sqrt{1+\eta^2}}}. \tag{14}$$

The wavefunction in Eq. 13 is used to calculate stable charge density and current density by Eq. 1

$$\begin{aligned}
\rho(x,y) &= eN^2 \sin^2[k_x(x+L_x)]\sin^2[k_y(y+L_y)] \\
&+eN^2\frac{\eta_x^2}{(1+\sqrt{1+\eta^2})^2}\cos^2[k_x(x+L_x)]\sin^2[k_y(y+L_y)] \\
&+eN^2\frac{\eta_y^2}{(1+\sqrt{1+\eta^2})^2}\sin^2[k_x(x+L_x)]\cos^2[k_y(y+L_y)], \\
j_x &= ec\frac{2\eta_y}{\sqrt{1+\eta^2}}\sin^2[k_x(x+L_x)]\sin[2k_y(y+L_y)], \\
j_y &= -ec\frac{2\eta_x}{\sqrt{1+\eta^2}}\sin^2[k_y(y+L_y)]\sin[2k_x(x+L_x)].
\end{aligned} \tag{15}$$

Both the charge density and the current density exhibit properties of a standing wave, characterized by the quantum numbers (n_x, n_y). As an example, we choose an excited state $(n_x = 2, n_y = 2)$ of a quantum well $(L_x = 10\text{ nm}, L_y = 10\text{ nm})$. Fig. 1 is the density plot of the charge expected for the behavior of an electron cloud. Fig. 2 is the density plot of the current density of the same electron, showing multiple vortices around the peaks of the electron cloud. The wave spin picture is further illustrated by the vector plot of the current in Fig. 3, which shows the circulation of each vortex in the same direction. It is clear that the wave spin in the excited state is distributed among multiple vortices that are holographic to each other. This topology suggests that each wave spin vortex represents a part or fraction of the total spin that can be studied and observed by interaction with an external field, as we will elaborate later.

In Fig. 3 it can also be seen that the current flows continuously along the edge of the quantum well. A similar behavior of the edge current is observed and studied in the quantum Hall effect [6] when a strong magnetic field is applied to topological insulator materials. The intrinsic edge current shown here suggests that topological spin effects can be observed even without the presence of any internal or external magnetic field.

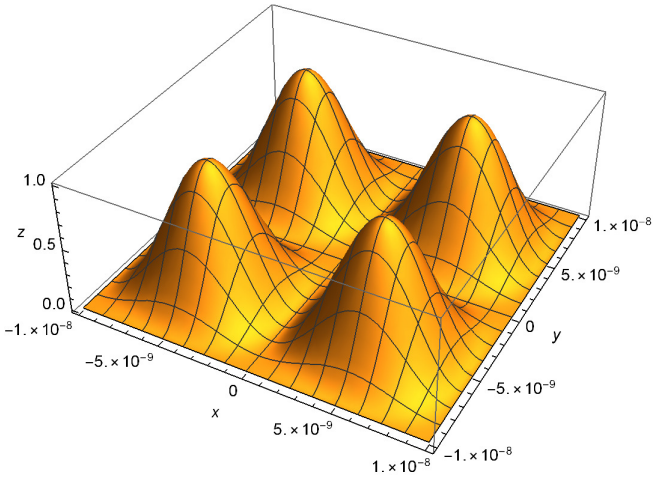

FIG. 1. Visualization of the electron charge by the charge density plot for a spin-up Dirac electron in the excited state $n_x = 2$ and $n_y = 2$ inside a quantum well of $L_x = 10$ nm and $L_y = 10$ nm. The z-axis represents the charge density of relative unit.

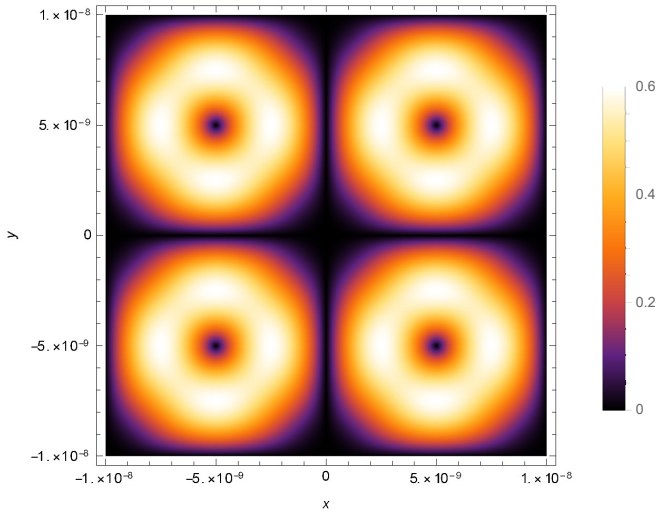

FIG. 2. Visualization of the electron spin by the current density plot for a spin-up Dirac electron in the excited state $n_x = 2$ and $n_y = 2$ inside a quantum well of $L_x = 10$ nm and $L_y = 10$ nm. The color chart represents the current density of relative unit.

III. TOPOLOGICAL CURRENT-FIELD INTERACTION

The electron spin interaction with a magnetic field is known to be $\frac{e}{m}\frac{\hbar}{2}\boldsymbol{\Sigma}\cdot\boldsymbol{B} = \mu_B\boldsymbol{\Sigma}\cdot\boldsymbol{B}$, where $\mu_B = \frac{e\hbar}{2m}$ is the Bohr magneton. Such expression excludes all geometrical and topological effects since $\boldsymbol{\Sigma}$ depicts a dimensionless point. Let us study the gauge-invariant spin-field interaction in Eq. 3,

$$\boldsymbol{j}\cdot\boldsymbol{A} = \Psi^\dagger(\boldsymbol{r},t)ec\boldsymbol{\alpha}\cdot\boldsymbol{A}(\boldsymbol{r})\Psi(\boldsymbol{r},t), \tag{16}$$

with the current density found in Eqs. 15 and a vector potential

$$\boldsymbol{A}(x,y) = \frac{B}{2}(-y,x,0) \tag{17}$$

representing a uniform magnetic field in the z-direction $\boldsymbol{\nabla}\times\boldsymbol{A}(x,y) = (0,0,B)$. Here we choose the symmetric gauge to describe the magnetic field. It can be verified that other gauges, such as the Landau gauge, yield the same result.

The interaction of Eq. 16 can now be evaluated by integrating over the entire quantum well to give the first-

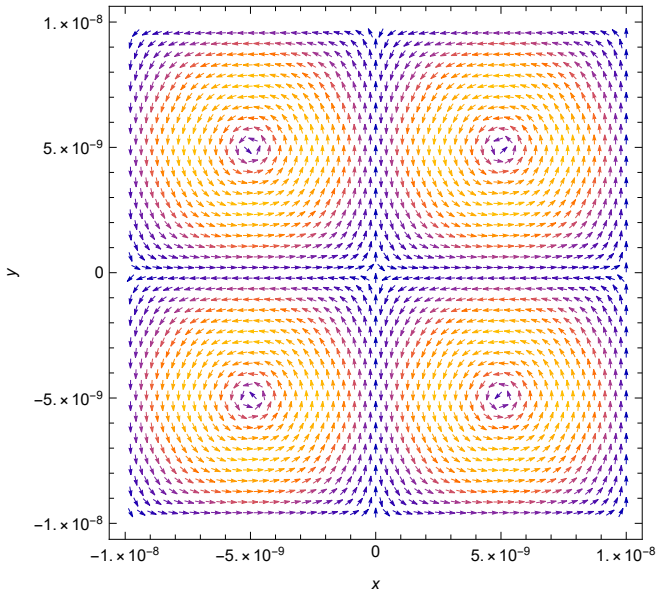

FIG. 3. Visualization of the electron spin by the current density vector plot for a spin-up Dirac electron in the excited state $n_x = 2$ and $n_y = 2$ inside a quantum well of $L_x = 10$ nm and $L_y = 10$ nm.

order energy shift by assuming a weak A field

$$\begin{aligned}\mathcal{E}^{(1)} &= \frac{1}{2L_x}\frac{1}{2L_y}\int_{-L_y}^{L_y}\int_{-L_x}^{L_x} \boldsymbol{j}\cdot\boldsymbol{A}(x,y)dxdy \\ &= \frac{e\hbar B}{2m\sqrt{1+\eta^2}} = \frac{\mu_B B}{\sqrt{1+\eta^2}},\end{aligned} \tag{18}$$

Thus, the difference between the spin-up and spin-down energy shifts becomes

$$\Delta\mathcal{E} = 2\mathcal{E}^{(1)} = \frac{2\mu_B B}{\sqrt{1+\eta^2}}, \tag{19}$$

which largely recovers the expression of the anomalous Zeeman splitting $2\mu_B B$, but modifies the expression by additional geometric factors and quantum numbers via Eq. 11. This indicates a finer structure of the anomalous Zeeman effect dependent on the geometric and topological properties of the current densities at different states.

Since spin is a wave property, its dimensions can be larger than that of the field, therefore its topological features can be probed by a confined field such as

$$\tilde{\boldsymbol{A}}(\boldsymbol{r}) = \begin{cases} \frac{B}{2}(-y+b, x-a, 0), & \begin{matrix} -L_x/2 < x-a < L_x/2, \\ -L_y/2 < y-b < L_y/2 \end{matrix} \\ 0, \text{ elsewhere}, \end{cases} \tag{20}$$

which is centred at (a, b) and only a quarter of the quantum well in size. The vector potential of Eq. 20 produces the same uniform magnetic field within the confined area. Fig. 4 shows the vector plot of such a field

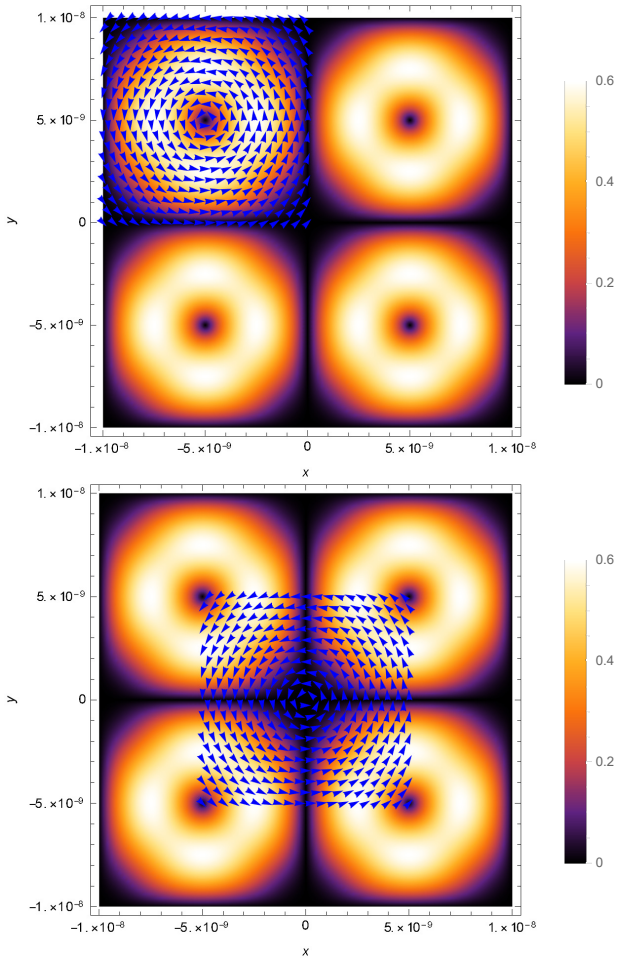

FIG. 4. Visualization of the electron spin interacting with an electromagnetic field confined to be smaller than the spin itself. The upper figure shows the magnetic potential (blue) of Eq. 20 overlapping with the upper left current vortex (red) at $a = -L_x/2, b = L_y/2$, producing a quarter spin-field interaction. The lower figure shows that the magnetic potential (blue) of Eq. 20 lies in the middle of the quantum well at $a = 0, b = 0$, producing a zero spin-field interaction.

superimposed on the electron current distribution. We now perform the same integration over the quantum well as in Eq. 18. We find that the current-field interaction depends on their relative positions. The interaction energy for $(n_x = 2, n_y = 2)$ is now

$$\begin{aligned}\mathcal{E}^{(1)}_{a,b} &= \frac{1}{2L_x}\frac{1}{2L_y}\int_{-L_y}^{L_y}\int_{-L_x}^{L_x} \boldsymbol{j}\cdot\tilde{\boldsymbol{A}}(x,y)dxdy \\ &= \begin{cases} \frac{1}{4}\frac{\mu_B B}{\sqrt{1+\eta^2}}, a = \pm L_x/2, b = \pm L_y/2 \\ 0, \quad a = 0, b = 0, \end{cases}\end{aligned} \tag{21}$$

which is only $\frac{1}{4}$ of the spin and magnetic field interaction in Eq. 18 when the field overlaps with one of the current vortices. The fractional spin effect is due to the partial participation of the wave spin represented by the current density. A special situation arises when the field lies at

the center of the quantum well. Then a zero interaction is observed, because equal fractions of the current flowing in different directions are exactly cancelled out.

In practice, such a minuscule magnetic field can be generated by a nano-sized current loop processed with modern lithography technology that produces a more realistic field potential without the sharp cut-off. However, the fractional spin effect remains observable. It is also possible to generate vortex optical fields [7] that can be focused on a smaller region than the quantum well. The electron spin can thus be studied and manipulated partially in order to gain full knowledge and control over the entire wave spin.

IV. CONCLUSIONS

In conclusion:

1. We argue that spin is not an abstract two-valued property of the electron particle but a property of the electron wave that can be fully described by its momentum and current densities.

2. We show that in the excited state, the current density of an electron forms multiple vortices in a magnetic field-free quantum well. The topology of these vortices depends on the quantum numbers of the states and is holographic in nature.

3. We investigate the anomalous Zeeman effect of the wave spin and show that the anomalous Zeeman splitting contains finer structures than those from the conventional particle spin picture.

4. We show that the geometrical and topological properties of the wave spin can be observed and studied through its interaction with an electromagnetic field comparable in size to the wave spin, where fractional spin effects can be observed.

V. DISCUSSIONS

Evidently, the discussion above could have implications on many spin-based applications, including spintronics, quantum computing, molecular biology etc., which merit fresh investigation with the wave picture of the spin. Here we offer some preliminary considerations.

1. In the field of quantum technology, the electron spin has been proposed as a candidate for use as a quantum bit (qubit), which is a superposition of the spin-up and spin-down states $\alpha \begin{pmatrix} 1 \\ 0 \end{pmatrix} + \beta \begin{pmatrix} 0 \\ 1 \end{pmatrix}$, where α and β are complex numbers. In the wave spin picture, the spin states $\begin{pmatrix} 1 \\ 0 \end{pmatrix}$ and $\begin{pmatrix} 0 \\ 1 \end{pmatrix}$ are replaced by the spinor wave functions, as in Eq. 13, where the spatial wave function serves as the spinor component. We have thus argued that the spin cannot be completely isolated from the physical environment that affects the wave. Any change of the boundary conditions alters the wave functions, and hence the spin states. We further argue that the spin cannot be completely isolated from the Hilbert space of the electron either, since each spatial state has its own unique spin state. Any transition to or from other spatial states alters the original spin state, leading to decoherence of the prepared qubit and loss of the quantum information. This means that additional protection and correction mechanisms need to be implemented to protect and preserve the spin qubit.

2. The multi-vortex wave spin topology and its partial interaction with electromagnetic fields show that the spin-field interaction is topologically and geometrically dependent, suggesting novel schemes for parallel information processing using spin. Each vortex of the current is a holographic part of the entire spin and can interact simultaneously with multiple electromagnetic fields, potentially enabling parallel computing. Such parallel quantum computer can be developed in principle by combining spintronic and vortex optic technologies.

3. It is conceivable that the holographic spin interactions could already exist in nature. It is suggested that the electron spin could play a role in bio-homochirality [8]. The wave spin perspective could provide insights and a path of solution of this fundamental biological mystery [9]. In more general terms the role of spin for a molecule deserves renewed investigation, since the wave spin could interact holographically with all atoms of the molecule via the spinning electron cloud, leaving a coherent spin footprint on the entire molecule.

VI. ACKNOWLEDGEMENT

The authors would like to thank Jora L. Gao for her careful review of the manuscript. The authors would also like to thank Jane Y. Gao and W. Wang for stimulating discussions on the role of spin in biology.

[1] J. Gao, J. Phys. Commun. **6**, 081001 (2022).
[2] F. J. Belinfante, Physica **6**, 887 (1939).
[3] F. J. Belinfante, Physica **7**, 449 (1940).
[4] H. C. Ohanian, Am. J. Phys. **54**, 6 (1986).

[5] L. Rosenfeld, Acad.Roy.Belg. Memoirs de Classes de Science **18**, 6 (1940).
[6] K. von Klitzing, T. Chakraborty, P. Kim, and et al, Nat Rev Phys **2**, 397–401 (2020).
[7] D. M. Fatkhiev, M. A. Butt, E. P. Grakhova, R. V. Kutluyarov, I. V. Stepanov, N. L. Kazanskiy, S. N. Khonina, V. S. Lyubopytov, and A. K. Sultanov, Recent advances in generation and detection of orbital angular momentum optical beams—a review, Sensors **21**, 10.3390/s21154988 (2021).
[8] W. Wang, Did bio-homochirality arise from spin-polarized electron?, 10.48550/ARXIV.2202.04808 (2022).
[9] J. Rivera Islas, J. C. Micheau, and T. Buhse, The origin of biomolecular chirality, in *Life in the Universe: From the Miller Experiment to the Search for Life on other Worlds*, edited by J. Seckbach, J. Chela-Flores, T. Owen, and F. Raulin (Springer Netherlands, Dordrecht, 2004) pp. 73–77.